Cloud Optics

ATMOSPHERIC AND OCEANOGRAPHIC SCIENCES LIBRARY

VOLUME 34

The titles published in this series are listed at the end of this volume.

Cloud Optics

by

Alexander A. Kokhanovsky

University of Bremen, Germany

Springer

A C.I.P. Catalogue record for this book is available from the Library of Congress.

ISBN-10 1-4020-3955-7 (HB)
ISBN-13 978-1-4020-3955-3 (HB)
ISBN-10 1-4020-4020-2 (e-book)
ISBN-13 978-1-4020-4020-7 (e-book)

Published by Springer,
P.O. Box 17, 3300 AA Dordrecht, The Netherlands.

www.springer.com

Printed on acid-free paper

Printed in the Netherlands.

To my parents

Since one must turn his eyes toward heaven to look at them, we think of them . . . as the throne of God . . . That makes me hope that if I can explain their nature . . . one will easily believe that it is possible in some manner to find the causes of everything wonderful about the Earth.

Rene Descartes

CONTENTS

FOREWORD

Clouds play an important role in the atmospheric radiative transfer and global water cycle. However, their properties are poorly understood. This is the main reason behind great efforts undertaken by the international research community to better understand cloud characteristics. Every year a lot of papers are published on various aspects of cloud research.

Optical remote sensing of clouds enables us to study cloud microphysical and geometrical characteristics using airborne, spaceborne, and ground-based optical instrumentation. Therefore, knowledge in the area of cloud optics is of great importance to any cloud physicist. Most important concepts of cloud optics and, in particular its theoretical basis, were formulated in 20th century. Time has come to summarize these concepts in a coherent way to establish a solid basis for cloud optics as a specific branch of physical optics in general.

Clouds are collections of droplets and crystals suspended in the air. Therefore, the main problem is to understand the laws of photon diffusion, scattering, absorption, and emission in a random collection of solid and liquid particles. The relationships of transmitted and reflected light fluxes with the geometrical and microphysical characteristics of clouds are of particular importance. Intuitively, one expects that the solar light transmittance by clouds decreases with cloud thickness. Also the cloud reflectance is larger for thicker clouds. Clearly, ice and liquid water absorption bands are present in spectral cloud reflectance as measured by the optical spectrometer orbiting the planet. However, what is the precise relationship of registered spectra and the cloud microstructure (e.g., the size of crystals and droplets)? The main aim of this book is to prepare the reader to deal with these and similar problems in a quantitative way. Therefore, we concentrate mostly on

theoretical cloud optics. The description of optical instruments is outside the scope of this book.

Cloud optics is based on electromagnetic theory and statistical physics. In particular, Maxwell equations are used to establish laws of scattering and absorption of a light beam by a single droplet or an ice crystal. This allows us to calculate characteristics of single light scattering in a cloudy medium. Then the laws of statistical physics are applied to study diffusion, absorption, emission, and multiple scattering of photons in clouds. In particular, the Boltzmann transport equation, often used in statistical physics, forms a basis for studies of multiple scattering effects in clouds.

The book consists of four Chapters. Chapter 1 presents a review of cloud microphysical and geometrical properties. The interaction of an electromagnetic wave with a single liquid or solid particle is the main subject of Chapter 2. Here, starting from Maxwell equations, light scattering angular distributions and absorption characteristics are calculated depending on the size and shape of a single particle or shape/size statistical distributions of noninteracting scatterers. The problem of multiple light scattering is presented in Section 3. We introduce the radiative transfer equation in its most general form valid for three-dimensional radiative transfer with account for the change of light polarization due to scattering and transport processes. Chapter 4 is devoted to the selected applications.

The author is grateful to J. P. Burrows, A. Macke, B. Mayer, V. V. Rozanov, W. von Hoyningen-Huene, and E. P. Zege for many stimulating discussions and cooperation.

Chapter 1

MICROPHYSICS AND GEOMETRY OF CLOUDS

1.1 Microphysical Characteristics of Clouds

1.1.1 Droplet Size Distributions

Water clouds consist of small liquid droplets suspended in air. Cloud droplets have a spherical shape in most cases, although particles of other shapes can exist due to various external influences. For instance, the deformation of large particles due to the gravitational force is of importance for raining clouds with droplets having radii 1 mm and larger. The average radius of droplets in non-precipitating water clouds is usually around 0.01 mm and the approximation of spherical particles works quite well (see Fig. 1.1).

Natural clouds with droplets of uniform size throughout the cloud volume never occur due to the variability of physical properties of air both in space and in time domains. Thus, one must consider the radius of a droplet a as a random value, which is characterized by the probability distribution function $f(a)$. This function is normalized by the following condition:

$$\int_0^\infty f(a)da = 1. \tag{1.1}$$

The integral

$$F(a) = \int_{a_1}^{a_2} f(a)da \tag{1.2}$$

gives the fraction of particles with radii between a_1 and a_2 in a unit volume of a cloud. The probability distribution function $f(a)$ can be represented as a

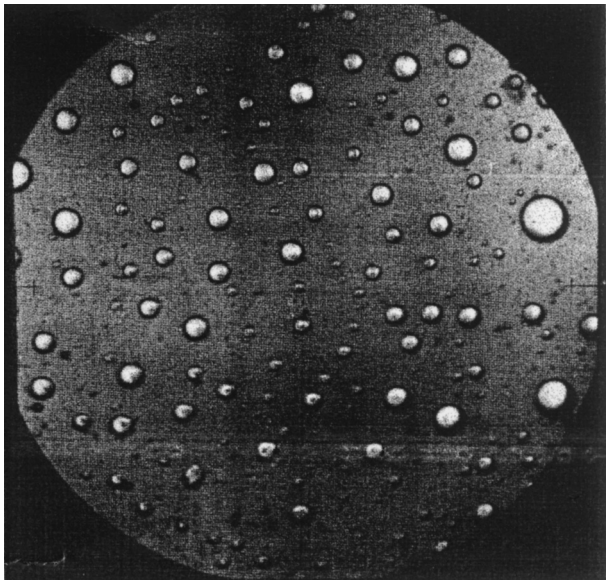

Fig. 1.1. A typical sample of cloud droplets caught on an oil slide and photographed under the microscope in an aircraft. The largest droplet has a radius of about 15 μm (Mason, 1975).

histogram, graphically or in a tabular form. However, it is most common to use an analytical form of this function, involving only one, two or three free parameters. This is, of course, a great simplification of real situations occurring in natural clouds, but most optical characteristics of a cloud only weakly depend on the fine structures of particle size distributions (PSDs) $f(a)$. McGraw et al. (1998) found that the local optical properties of polydispersions can be modelled with high accuracy by just the first six moments of the PSD. The usage of certain combinations of moments can reduce the number of parameters even further.

In most cases, the experimentally measured function $f(a)$ can be well represented by the gamma distribution (Deirmendjian, 1969):

$$f(a) = \mathbb{N} a^{\mu} e^{-\mu(a/a_0)}, \tag{1.3}$$

where

$$\mathbb{N} = \frac{\mu^{\mu+1}}{\Gamma(\mu+1) a_0^{\mu+1}} \tag{1.4}$$

is the normalization constant and $\Gamma(\mu+1)$ is the gamma function. It follows from Eq. (1.3) that the first derivative $f'(a_0) = 0$ and the second derivative $f''(a_0) < 0$. This means that the function $f(a)$ has the maximum at $a = a_0$. Equation (1.4)

follows from Eqs. (1.1) and (1.3) and the definition of the gamma function:

$$\Gamma(\mu) = \int_0^\infty x^{\mu-1} e^{-x} dx. \tag{1.5}$$

In particular, one derives at integer $\mu \geq 1 : \Gamma(\mu) = (\mu - 1)!$. The parameter μ characterizes the width of the PSD $f(a)$, being smaller for wider distributions. Moments

$$\langle a^n \rangle = \int_0^\infty a^n f(a) da \tag{1.6}$$

of the PSD (1.3) can be found analytically:

$$\langle a^n \rangle = \left(\frac{a_0}{\mu}\right)^n \frac{\Gamma(\mu + n + 1)}{\Gamma(\mu + 1)}. \tag{1.7}$$

Equation (1.7) is used to find the average volume of spherical droplets

$$\langle V \rangle = \frac{4\pi}{3} \int_0^\infty a^3 f(a) da, \tag{1.8}$$

the average surface area

$$\langle \Sigma \rangle = 4\pi \int_0^\infty a^2 f(a) da, \tag{1.9}$$

and the average mass of droplets

$$\langle W \rangle = \rho \langle V \rangle, \tag{1.10}$$

where $\rho = 1$ g/cm^3 is the density of water. It follows that

$$\langle V \rangle = \frac{\Gamma(\mu + 4)}{\mu^3 \Gamma(\mu + 1)} v_0, \tag{1.11}$$

$$\langle \Sigma \rangle = \frac{\Gamma(\mu + 3)}{\mu^2 \Gamma(\mu + 1)} s_0, \tag{1.12}$$

$$\langle W \rangle = \frac{\Gamma(\mu + 4)}{\mu^3 \Gamma(\mu + 1)} w_0, \tag{1.13}$$

where

$$v_0 = \frac{4\pi a_0^3}{3}, s_0 = 4\pi a_0^2, w_0 = \rho v_0 \tag{1.14}$$

are corresponding parameters for a droplet having the radius a_0. In the case of the most often employed cloud PSD given by Eq. (1.3) with $a_0 = 4\mu$m and $\mu = 6$ [Cloud C1 model (Deirmendjian, 1969)] one can obtain:

$$\langle V \rangle = \frac{7}{3} v_0, \langle \Sigma \rangle = \frac{14}{9} s_0, \langle W \rangle = \frac{7}{3} w_0, \tag{1.15}$$

where $v_0 \approx 2.7 \times 10^{-16}\,\mathrm{m}^3$, $s_0 \approx 2 \times 10^{-12}\,\mathrm{m}^2$, $w_0 \approx 2.7 \times 10^{-10}\,\mathrm{g}$. Although parameters (1.14) are small, very large numbers of cloud droplets (typically, 100 particles in cm^3) create important factors for atmospheric processes.

Equation (1.3) allows to characterize the cloud droplet distribution by only two parameters: a_0 and μ. However, it should be remembered that neither a_0 nor μ is constant. They vary inside a cloud. Thus, a_0 and μ depend on the averaging scale, with large averaging scales producing more broad PSDs (with smaller values of μ). The value of $\mu = 2$ was found to be rather representative (Khrgian and Mazin, 1952) and this number is advised to be used in low resolution cloud satellite retrieval algorithms. It follows in this case: $f(a) = 8a_0^{-3}a^2 \exp(-2a/a_0)$ or $f(a) = a^2 \exp(-a)$ (in $\mu\mathrm{m}^{-1}$ if a is measured in μm) at $a_0 = 2\,\mu$m. This function reaches a maximum at $a_0 = 2\,\mu$m and then decreases exponentially as $a \to \infty$.

The parameter $\mu = 6$ (Deirmendjian, 1969), used in the derivation of Eq. (1.15), is typical only for small averaging scales (Fomin and Mazin, 1998). General features of the droplet spectra in water clouds were studied experimentally in great detail by Warner (1973).

Parameters a_0 and μ are defined in terms of the specific unimodal cloud droplet distribution (1.3). It is more lucrative to characterize cloud PSDs by their moments. Moments can be retrieved from optical measurements without reference to specific distribution laws (McGraw et al., 1998).

The effective radius (Hansen and Travis, 1974)

$$a_{ef} = \frac{\langle a^3 \rangle}{\langle a^2 \rangle} \tag{1.16}$$

is one of the most important parameters of any PSD. It is proportional to the average volume/surface ratio of droplets. The parameter (1.16) can be defined for non-spherical particles as well. The coefficient of variance (CV) of the PSD

$$C = \frac{\Delta}{\langle a \rangle} \tag{1.17}$$

where

$$\Delta = \sqrt{\int_0^\infty (a - \langle a \rangle)^2 f(a) da}, \tag{1.18}$$

is also of importance, especially for narrow droplet distributions. The value of Δ is called the standard deviation. The CV, which is equal to the ratio of the standard deviation to the mean radius $\langle a \rangle$, is often expressed in percent.

It follows for the PSD (1.3):

$$a_{ef} = a_0 \left(1 + \frac{3}{\mu}\right), \mathrm{C} = \frac{1}{\sqrt{1+\mu}} \tag{1.19}$$

and, therefore,

$$\mu = \frac{1}{C^2} - 1, a_0 = \frac{1 - C^2}{1 + 2C^2} a_{ef}. \tag{1.20}$$

The effective radius a_{ef} is always larger than the mode radius a_0. For instance, we obtain at $\mu = 3$: $a_{ef} = 2a_0$, C = 0.5, $\Delta = \langle a \rangle / 2$. Therefore, the standard deviation is equal to half of average radius at $\mu = 3$.

Equation (1.20) gives the meaning of the parameter μ in the PSD (1.3). In particular, we have as $C \to 0 : \mu \to \infty$. In situ measurements show that the value of a_0 often varies from 4 to 20 μm (Mason, 1975) and that $\mu \in [2, 8]$ in most cases. It should be pointed out that clouds with smaller droplets are not stable due to coagulation and condensation processes. Larger particles cannot reside in the terrestrial atmosphere for a long time due to the gravity force. Thus, several physical processes lead to the existence of the most frequent mode radius range. One can obtain from Eq. (1.19) and inequality $2 \leq \mu \leq 8$ that the value of $C \in [0.3, 0.6]$. Thus, it follows that the standard deviation of the radius of particles in water droplets is usually 30–60% of an average radius. Smaller and larger values of C do occur but values of C smaller than 0.1 were never observed (Twomey, 1977). Larger values of C may indicate the presence of the second mode in the range of large particles (Ayvazyan, 1991).

Equation (1.19) and results for a_0 and μ just reported lead to the effective radius a_{ef} of water droplets being in the range from 5 to 50 μm, depending on the cloud type. Near-global survey of the value of a_{ef}, using satellite data, shows that typically 5 μm $\leq a_{ef} \leq$ 15 μm (Han et al., 1994). We see that water clouds with $a_{ef} > 15$ μm are rare. This can be used to discriminate satellite pixels with ice crystals even at wavelengths where ice and water absorption coefficients are almost equal. Such a possibility of discrimination is due to much larger (e.g., in 5–10×) effective sizes of ice crystals as compared to droplets. The large size of ice crystals will reduce the reflection function in near infrared considerably as compared to droplets. This reduction can be easily detected. Note that clouds with $a_{ef} > 15$ μm are often raining (Masunaga et al., 2002). Pinsky and Khain (2002) showed that the threshold of the occurrence of drizzle is around $a_{ef} > 15$ μm. Then strong collisions of droplets start. The vertical extent and the thermodynamic state of clouds also influences the probability of precipitation.

Some authors prefer to use the representation of the PSD by the following analytical form (Ayvazyan, 1991):

$$f(a) = \frac{1}{\sqrt{2\pi}\sigma a} \exp\left(-\frac{\ln^2(a/a_m)}{2\sigma^2}\right), \tag{1.21}$$

which is called the log-normal distribution. The relations between values of a_{ef}, $\langle a \rangle$, Δ and parameters of the gamma and log-normal PSDs are presented

Table 1.1. Particle size distributions and their characteristics.

$f(a)$	B	$\langle a \rangle$	a_{ef}	C
Gamma distribution $Ba^{\mu}e^{-\mu(a/a_0)}$	$\dfrac{\mu^{\mu+1}}{a_0^{\mu+1}\Gamma(\mu+1)}$	$a_0\left(1+\dfrac{1}{\mu}\right)$	$a_0\left(1+\dfrac{3}{\mu}\right)$	$\sqrt{\dfrac{1}{\mu+1}}$
Log-normal distribution $\dfrac{B}{a}\exp\left(-\dfrac{\ln^2(a/a_m)}{2\sigma^2}\right)$	$\dfrac{1}{\sqrt{2\pi}\sigma}$	$a_m e^{0.5\sigma^2}$	$a_m e^{2.5\sigma^2}$	$\sqrt{e^{\sigma^2}-1}$

in Table 1.1. The value of Δ_{ef} in this table represents the effective variance, defined as:

$$\Delta_{ef} = \frac{\int_0^\infty (a - a_{ef})^2 a^2 f(a) da}{a_{ef}^2 \int_0^\infty a^2 f(a) da}. \tag{1.22}$$

This parameter is often used instead of the coefficient of variance C (Hansen and Travis, 1974) because of a special importance attached to the value of the effective radius of droplets a_{ef} as compared to the average radius $\langle a \rangle$ for the problems of cloud optics. For instance, light extinction in clouds is governed mostly by values of a_{ef} and liquid water content (LWC) independently of the type of PSD $f(a)$ (Kokhanovsky, 2004a). PSDs (1.3) and (1.21) at $a_{ef} = 6$ μm and $C = 0.38$ are shown in Fig. 1.2. Then it follows: $a_0 = 4$ μm, $\mu = 6$, $a_m = 5.6$ μm, $\sigma = 0.3673$.

The influence of μ on the PSD (1.3) is shown in Fig.1.3 at $\mu = 2, 6, 8$ and $a_{ef} = 6$ μm. Light extinction in media having droplet size distributions shown in Figs. 1.2 and 1.3 (and the same LWC) will be almost identical although PSDs are quite different.

Particle number concentration, N, in addition to particle size and shape, is of importance for the propagation, scattering and extinction of light in cloudy media. The value of N gives the number of particles in a unit volume and is expressed in cm^{-3}. It is usually in the range 50–1000 cm^{-3} (Fomin and Mazin, 1998). Clearly, the concentration of droplets depends on the concentration C_N of atmospheric condensation nuclei. The value of C_N is smaller over oceans than over continents, so the concentration of droplets in marine clouds is on average smaller than over continents. Generally, the smaller concentration of droplets over oceans means that they can grow larger, producing clouds with larger droplets over oceans, which is confirmed by the analysis of satellite optical imagery as well (Han et al., 1994). This influences the occurrence and the rate of precipitation.

Svensmark and Friis-Christensen (1997) and Marsh and Svensmark (2000) have speculated that cosmic ray ionization could influence the production of

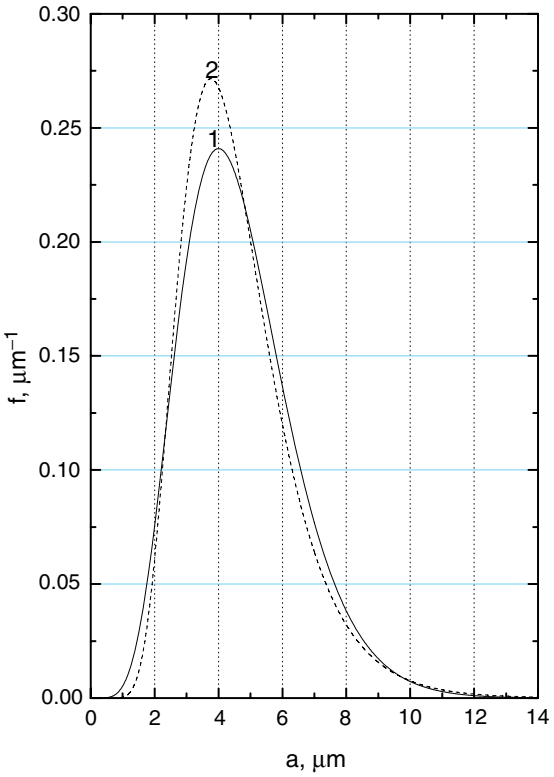

Fig. 1.2. Particle size distributions (1-gamma distribution, 2-log-normal distribution).

condensation nuclei and, therefore, cloud properties. This is of importance for climate change problems as discussed by Svensmark (1998).

The dimensionless volumetric concentration of droplets $C_v = N\langle V\rangle$ and LWC $C_w = \rho C_v$ or [see Eq. (1.10)] $C_w = N\langle W\rangle$ are often used in cloud studies as well. The value of C_w is usually in the range 0.01–1.0 gm^{-3} with typical values of 0.1 gm^{-3}. Therefore, the most frequent values of C_v are in the range of $[10^{-7}, 10^{-5}]$. This means that only a very small fraction of a cloud volume is occupied by droplets. This simplifies the solution of many cloud optics problems. In particular, local cloud optical characteristics can be calculated not accounting for the close-packed media effects (Kokhanovsky, 2004a). Numbers given above are representative, but it should be remembered that these values can change in a broader range in real situations. The LWC is not constant throughout a cloud but has larger values near the top of a cloud in most cases (Feigelson, 1981). This is illustrated in Fig. 1.4. Such a behaviour is characteristic for a_{ef} as well (see Fig. 1.5).

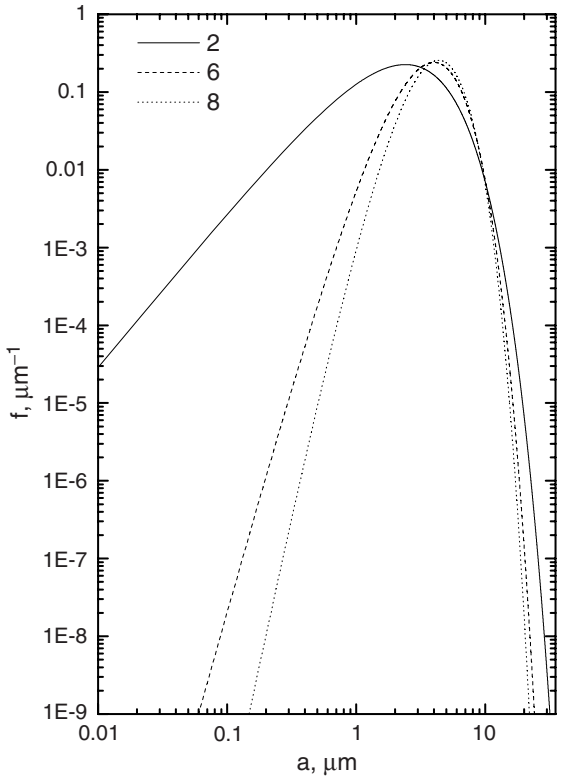

Fig. 1.3. Gamma particle size distributions for various μ at $a_{ef} = 6$ μm.

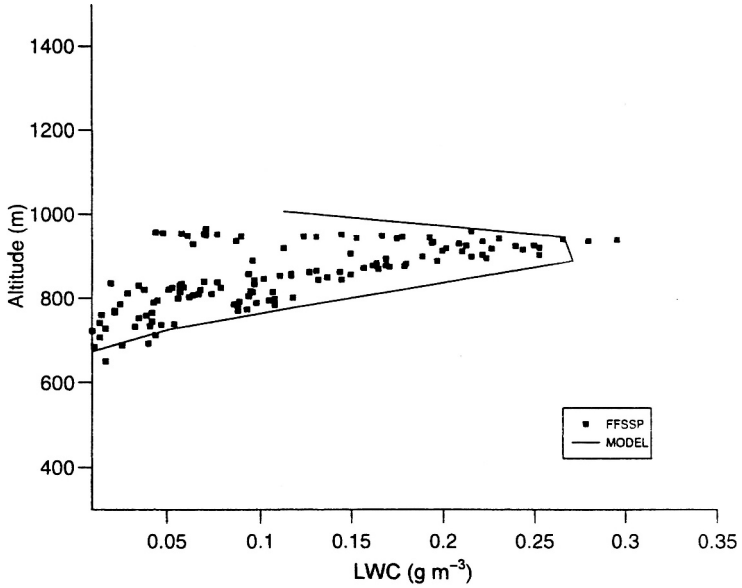

Fig. 1.4. Squares give measured values of the LWC as the function of altitude. Line gives the modelled LWC-profile. Further details are given by Ghosh et al. (2000).

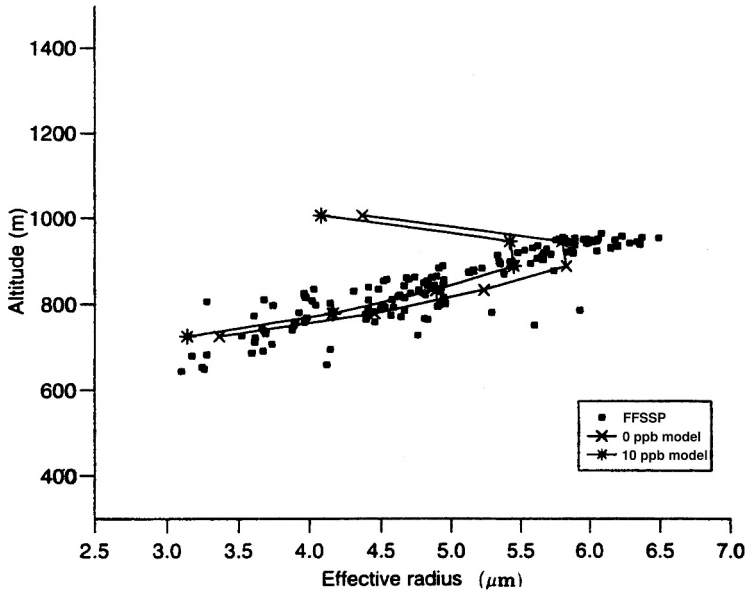

Fig. 1.5. Squares give measured values of the effective radius as the function of altitude. Line gives the modelled profile of the effective radius assuming different concentrations of HNO_3 acid in a cloud layer. Further details are given by Ghosh et al. (2000).

The liquid water path (LWP) w is defined as

$$w = \int_{z_1}^{z_2} C_w(z)dz, \tag{1.23}$$

where z_1 is the cloud bottom height and z_2 is the cloud top height, $l = z_2 - z_1$ is the geometrical thickness of a cloud. It follows at $C_w = \text{const}$:

$$w = C_w l. \tag{1.24}$$

The geometrical thickness of clouds varies, depending on the cloud type. It is in the range of 500–1000 m for stratocumulus clouds in most cases. Near-global data obtained by Han et al. (1994) from satellite measurements show that the LWP w is typically in the range of 50–150 g/m^2. The annual mean is equal to 86 g/m^2 (Han et al., 1994). Then we have at the cloud geometrical thickness $l = 860$ m: $C_w = 0.1$ g/m^3, which is a typical value of the LWC in water clouds (see Tables 1.2, 1.3 and Fig. 1.4). It should be underlined that remotely sensed values of the LWP and a_{ef} depend on the scale of horizontal averaging and also on the assumptions used in the retrieval procedures (see Figs. 1.6 and 1.7). Annual and monthly means of the LWP and a_{ef} over the globe in combination with many other cloud parameters derived from satellite data can be found at http://isccp.giss.nasa.gov/products/browsed2.html (Rossow and Schiffer, 1999).

Table 1.2. Geometrical and microphysical characteristics of marine water clouds obtained using experimental measurements (Miles et al., 2004).

B	T	H	N	LWC	a_{ef}	C	a_0	μ	a_m	σ
630	860	650	50	0.15	9.50	25.60	7.88	14.6	8.20	0.24
630	860	750	45	0.23	11.5	28.28	9.12	11.5	9.60	0.27
630	860	850	45	0.35	13.4	31.11	10.2	9.50	10.8	0.29
800	1000	900	75	0.28	11.2	49.69	6.53	4.20	7.55	0.40
800	1000	1000	100	0.49	13.0	44.00	6.16	2.70	7.70	0.46
240	760	240	23	0.01	5.75	42.50	2.97	3.20	3.60	0.43
240	760	440	56	0.13	8.95	32.00	6.82	9.60	7.25	0.29
240	760	620	111	0.37	9.80	27.59	8.29	16.5	8.55	0.23
—	—	—	91	0.18	7.95	15.13	7.44	43.6	7.50	0.15
—	—	1300	66	0.13	8.20	23.33	7.28	23.6	7.05	0.19
—	—	1300	22	0.03	7.60	30.53	6.10	12.2	6.40	0.26
610	960	700	160	0.09	6.00	43.68	3.50	4.20	4.05	0.40
610	960	800	182	0.31	8.00	29.20	6.27	10.9	6.60	0.28
610	960	930	158	0.47	9.60	28.31	7.63	11.6	8.00	0.27
1290	1460	1310	107	0.03	4.30	32.39	3.11	7.80	3.35	0.32
1290	1460	1340	142	0.06	5.10	30.59	3.87	9.40	4.15	0.29
1290	1460	1390	143	0.14	6.65	28.95	5.26	11.4	5.55	0.27
1290	1460	1430	140	0.22	7.65	98.54	6.47	16.5	6.70	0.23
—	—	310	12	0.02	7.75	44.25	4.69	4.60	5.30	0.39
—	—	380	5	0.004	7.20	47.92	3.48	2.80	4.35	0.45
420	730	460	28	0.08	9.90	42.48	6.74	6.40	7.40	0.34
420	730	530	39	0.13	11.2	55.70	5.95	3.40	7.20	0.42
420	730	610	59	0.2	11.3	60.14	5.46	2.80	6.80	0.45
420	730	690	73	0.17	11.0	69.23	3.48	1.40	5.30	0.54
380	830	480	79	0.16	8.90	40.00	5.68	5.30	6.35	0.37
380	830	730	94	0.59	12.5	33.65	9.58	10.0	10.1	0.24
408	684	575	296	0.22	6.45	41.67	4.00	4.90	4.65	0.35
408	684	682	228	0.29	7.75	41.74	4.77	4.80	5.35	0.39
410	740	410	116	0.04	4.75	22.35	3.95	14.8	4.10	0.24
410	740	580	123	0.29	9.00	29.61	6.86	9.60	7.30	0.29
410	740	740	149	0.35	9.80	33.75	6.86	7.00	7.60	0.32
1680	2350	1770	58	0.07	7.50	38.79	4.94	5.80	5.45	0.36
1680	2350	1890	40	0.08	9.00	40.74	5.63	5.00	6.35	0.38
1680	2350	240	30	0.10	12.0	60.00	4.50	1.80	6.30	0.51
1680	2350	2200	26	0.09	12.2	60.28	4.41	1.70	6.35	0.51
1310	1980	1250	40	0.12	10.4	42.48	6.24	4.50	7.15	0.38
1310	1980	1400	32	0.12	11.7	49.68	5.95	3.10	7.20	0.44
1310	1980	1620	52	0.26	12.2	40.98	7.63	5.00	8.60	0.37
1310	1980	1830	35	0.15	12.1	47.59	6.43	3.40	7.65	0.43

The meaning of columns as follows: B(m): cloud base height; T(m): cloud top height; H(m): height of measurements; N: droplet number concentration (cm^{-3}); LWC: liquid water content (gm^{-3}); a_{ef}: effective radius (μm); C: coefficient of variance; a_0: mode radius (μm) for the gamma PSD (1.3); μ: half-width parameter of the gamma PSD (1.3); and a_m (μm) and σ are parameters of the log-normal PSD (1.21).

Table 1.3. Geometrical and microphysical characteristics of continental water clouds obtained using experimental measurements (Miles et al., 2004).

B	T	H	N	LWC	a_{ef}	C	a_0	μ	a_m	σ
310	—	320	21	0.0038	4.15	46.55	2.29	3.7	2.70	0.41
350	—	360	59	0.0025	2.35	30.77	1.74	8.6	1.85	0.31
360	—	370	12	0.003	4.40	53.57	2.04	2.6	2.55	0.46
400	—	410	147	0.0093	2.75	32.65	1.77	5.4	2.00	0.36
400	—	410	228	0.0137	2.55	28.57	1.81	7.3	1.95	0.33
630	870	675	350	0.22	5.75	29.59	4.48	10.6	4.75	0.28
630	870	750	285	0.28	6.70	30.09	5.15	10.0	5.45	0.29
630	870	850	270	0.6	8.50	22.73	7.31	18.5	7.55	0.22
808	1040	908	480	0.12	4.20	27.03	3.49	14.8	3.60	0.24
808	1040	990	260	0.13	5.35	30.43	4.25	11.7	4.45	0.27
808	1040	908	370	0.13	4.65	31.25	3.68	11.5	3.90	0.27
808	1040	990	190	0.09	5.45	39.53	3.83	7.1	4.15	0.33
250	530	250	15	0.02	10.0	70.00	1.67	0.6	3.85	0.62
250	530	390	35	0.08	11.4	76.85	2.62	0.9	4.85	0.58
300	630	470	40	0.11	12.7	83.04	2.12	0.6	5.00	0.61
1350	2250	1800	148	0.4	9.15	26.38	7.73	16.3	8.00	0.23
—	—	800	215	0.01	2.60	58.06	1.65	5.2	1.85	0.37
—	—	800	418	0.12	2.25	46.88	1.32	4.3	1.50	0.40
800	1000	1000	250	0.2	6.50	37.25	4.38	6.2	4.80	0.35
380	790	440	60	0.003	3.05	38.46	1.18	1.9	1.65	0.50
380	790	550	366	0.06	4.20	48.21	1.20	2.7	2.45	0.46
380	790	650	401	0.11	4.85	48.48	2.50	3.2	3.05	0.43
380	790	750	396	0.15	5.40	50.68	2.83	3.3	3.40	0.43
1430	2010	1700	190	0.3	9.00	53.51	4.09	2.5	5.20	0.47
1430	2010	1700	450	0.7	7.70	27.61	6.20	12.5	6.50	0.26
1750	1870	1815	220	0.24	7.50	44.44	4.33	4.1	5.00	0.40
1750	1870	1815	200	0.035	4.00	41.67	2.48	4.9	2.80	0.38
450	673	571	693	0.2	5.25	57.14	2.1	2.0	2.80	0.50
450	673	673	575	0.26	6.25	61.97	2.17	1.6	3.25	0.51
750	1090	750	160	0.03	3.85	30.77	2.95	9.8	3.15	0.29
750	1090	870	225	0.1	5.05	26.67	4.21	15.1	4.35	0.24
750	1090	950	165	0.19	6.75	21.77	5.95	22.2	6.10	0.20
750	1090	1040	310	0.41	7.20	25.58	6.04	15.7	6.30	0.24
820	1010	840	680	0.08	3.30	26.32	2.68	13.0	2.80	0.26
820	1010	925	440	0.17	4.75	24.42	4.05	17.3	4.15	0.23
820	1010	980	297	0.16	5.40	28.42	4.41	13.3	4.60	0.25
400	1210	480	80	0.09	7.15	31.93	5.28	8.5	5.65	0.31
400	1210	890	320	0.67	8.25	21.71	7.21	20.8	7.45	0.21
400	1210	1120	360	1.00	9.05	20.96	8.00	22.9	8.20	0.20
2470	2990	2710	96	0.1	7.00	34.51	4.94	7.2	5.35	0.33
2470	2990	2790	103	0.18	8.40	37.12	5.72	6.4	6.30	0.34
2470	2990	2870	93	0.28	10.0	35.63	7.00	7.0	7.60	0.33

(continued)

Table 1.3. *Continued*

B	T	H	N	LWC	a_{ef}	C	a_0	μ	a_m	σ
2470	2990	2940	106	0.41	10.8	34.29	7.74	7.6	8.35	0.32
2470	2990	3020	96	0.45	12.0	41.57	7.38	4.8	8.35	0.38
200	500	430	139	0.14	7.75	57.73	3.52	2.5	4.45	0.47
1460	1940	1750	494	0.3	6.45	49.41	3.11	2.8	3.85	0.45
1460	1940	1840	432	0.33	6.80	48.91	3.51	3.2	4.25	0.43
1460	1940	1940	139	0.14	8.00	60.22	3.00	1.8	4.20	0.51

The meaning of columns as follows: B(m): cloud base height; T(m): cloud top height; H(m): height of measurements; N: droplet number concentration (cm^{-3}); LWC: liquid water content (gm^{-3}); a_{ef}: effective radius (μm); C: coefficient of variance; a_0: mode radius (μm) for the gamma PSD (1.3); μ: half-width parameter of the gamma PSD (1.3); and a_m (μm) and σ are parameters of the log-normal PSD (1.21).

Miles et al. (2000) summarized *in situ*—derived experimental data for various cloud parameters including N, a_{ef}, C_w, a_0, μ, a_m and σ. Some of them are shown in Tables 1.2–1.4 separately for marine and continental clouds. Correspondent frequency histograms are shown in Figs. 1.8–1.15. Also the correlation plot of LWC and N is given in Fig. 1.16 both for marine and continental clouds. We see that there is no important correlation between these parameters although continental

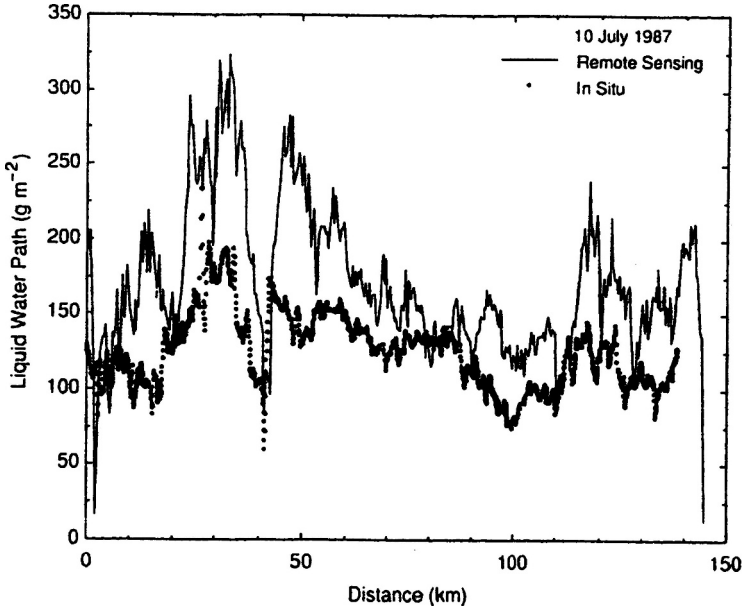

Fig. 1.6. Comparison of the liquid water path as a function of distance along the nadir track of the ER-2 as derived from remote sensing (solid line) and in situ measurements (solid circles) (Nakajima et al., 1991).

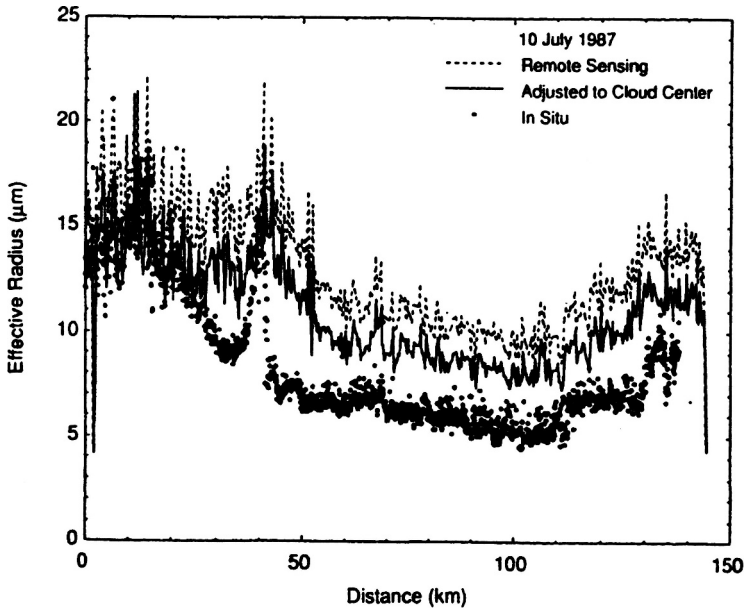

Fig. 1.7. Comparison of the effective radius as a function of distance along the nadir track of the ER-2 as derived from remote sensing (dashed line) and in situ measurements (solid circles) (Nakajima et al., 1991).

clouds have larger values of N. Similar results for values of a_{ef}, C are shown in Fig. 1.17. It follows that marine clouds have larger droplets, which is consistent with results shown in Fig. 1.16. Clearly, droplets have more chances to attract water molecules for smaller N. The frequently used cloud model C1 of Deirmendjian (1969) with $a_{ef} = 6$ μm and $\mu = 6(C = 1/\sqrt{7})$ is given by a circle in Fig. 1.17. We see that this model represents average cloud properties quite well. The analysis of Table 1.4 shows that the model is less accurate for marine clouds. So in addition

Table 1.4. Summary of results given in Tables 1.2 and 1.3 for average values of correspondent cloud parameters.

The cloud parameter	Continental clouds	Marine clouds	Average
a_{ef}, μm	6.0	9.0	7.5
C, %	44.0	43.0	43.5
N, cm^{-3}	254.0	91.0	172.5
LWC, gm^{-3}	0.20	0.17	0.185
a_0, μm	4.0	6.0	5.0
μ	7.0	8.0	7.5
a_m, μm	4.0	6.0	5.5
σ	0.4	0.4	0.4

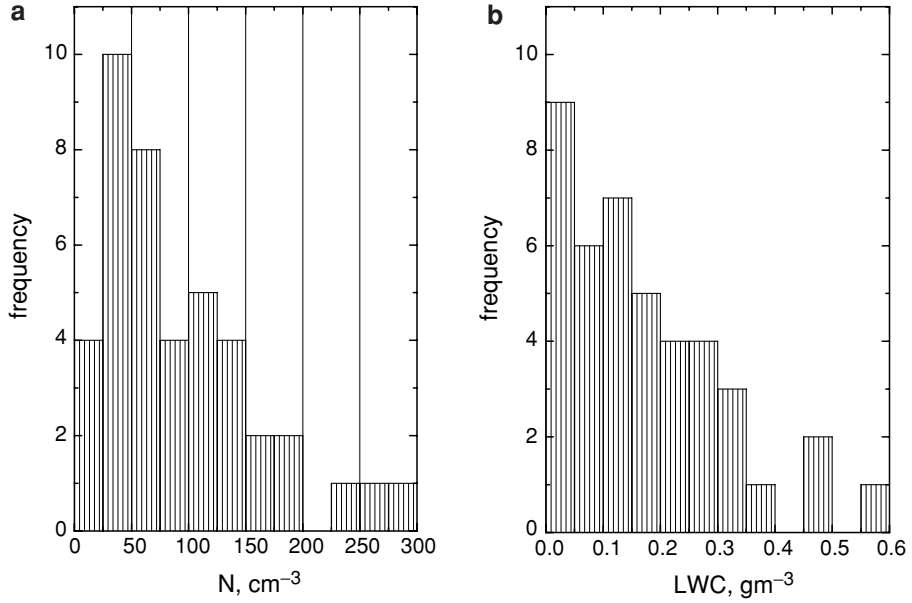

Fig. 1.8. Frequency distribution of N (a) and LWC (b) for marine water clouds obtained analysing multiple experimental measurements at different places and by different instruments and research groups (Miles et al., 2000).

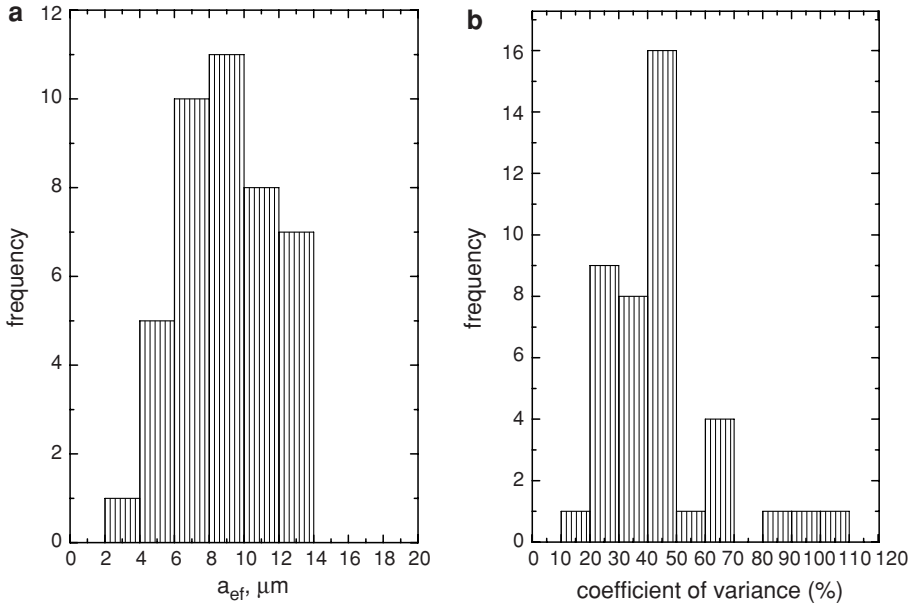

Fig. 1.9. The same as in Fig. 1.8 except for a_{ef} (a) and C (b).

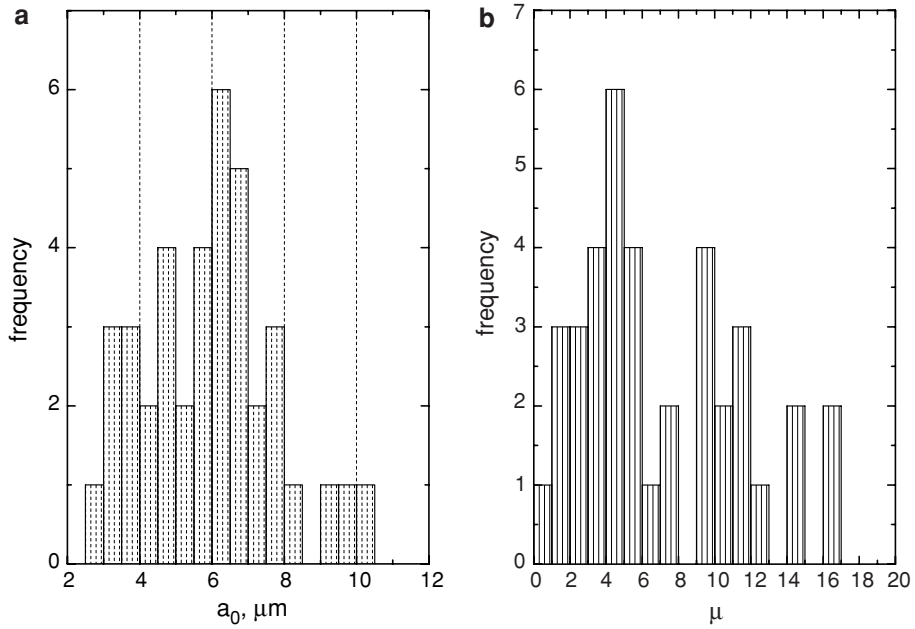

Fig. 1.10. The same as in Fig. 1.8 except for a_0 (a) and μ (b).

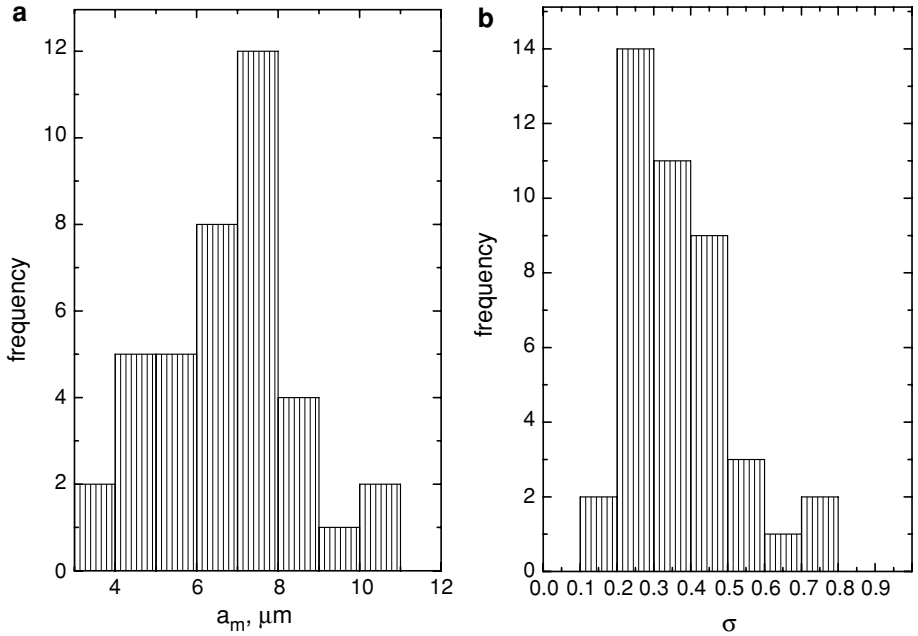

Fig. 1.11. The same as in Fig. 1.8 except for a_m (a) and σ (b).

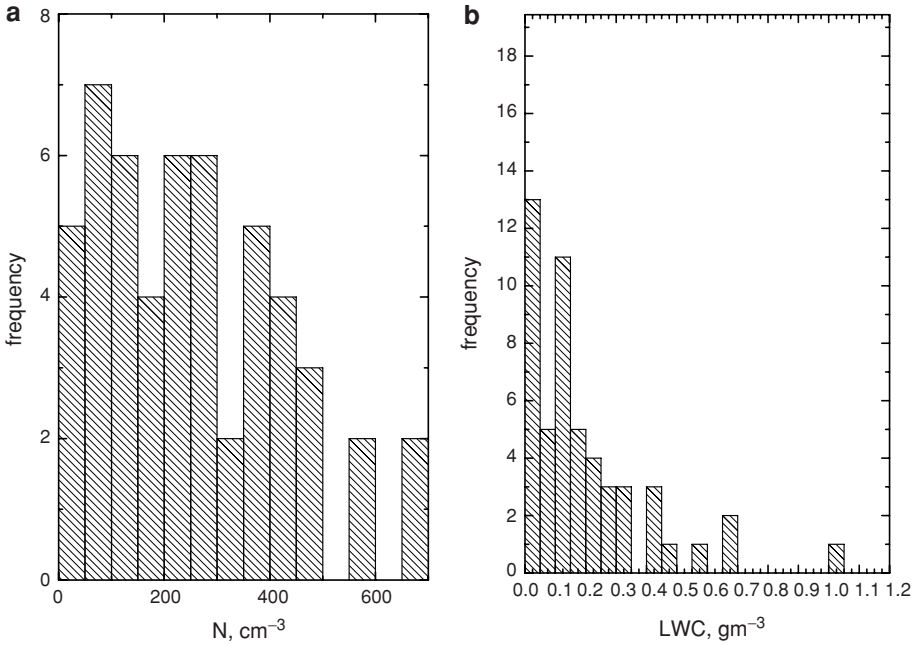

Fig. 1.12. Frequency distribution of N (a) and LWC (b) for continental water clouds obtained analysing multiple experimental measurements at different places and by different instruments and research groups (Miles et al., 2000).

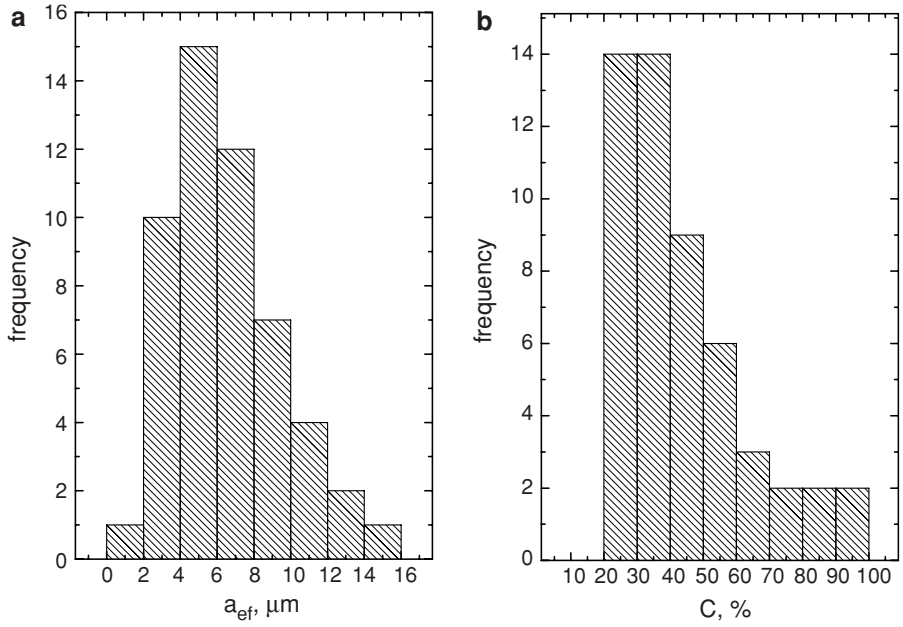

Fig. 1.13. The same as in Fig. 1.12 except for a_{ef} (a) and C (b).

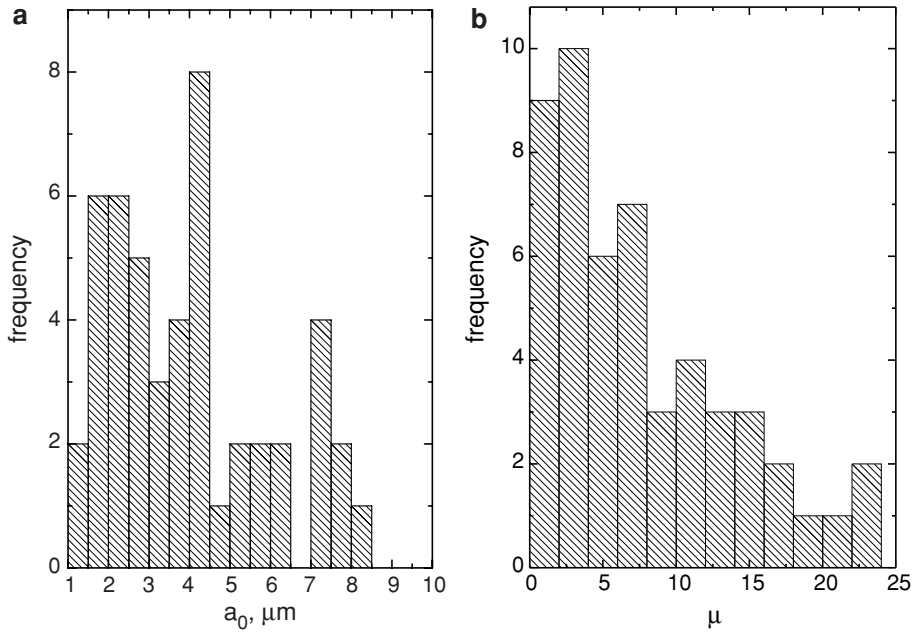

Fig. 1.14. The same as in Fig. 1.12 except for a_0 (a) and μ (b).

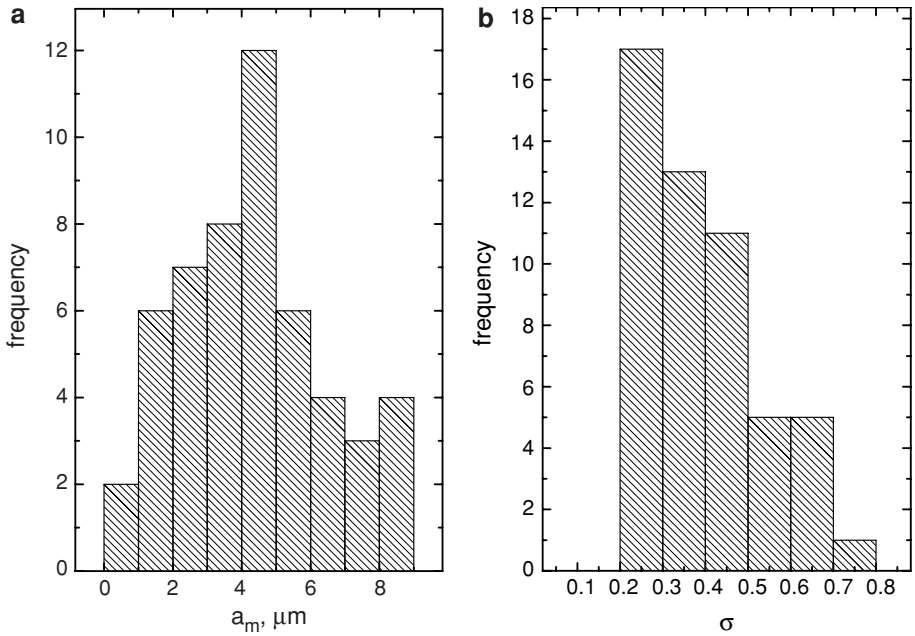

Fig. 1.15. The same as in Fig. 1.12 except for a_m (a) and σ (b).

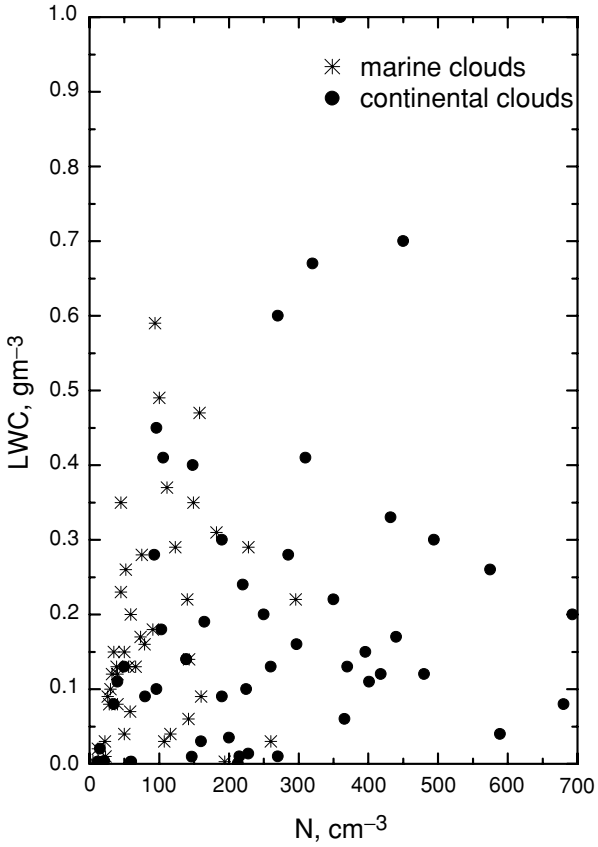

Fig. 1.16. The correlation between values of LWC and N for marine and continental clouds.

to the Deimendjian's continental cloud model (CCM), we propose also the marine cloud model (MCM) with the radius $a_0 = 6$ μm and $N = 100\,\mathrm{cm}^{-3}$ (see Table 1.5). We choose the parameter $\mu = 6$ for the marine model because it provides physically plausible dependence of the PSD on V at small values of V : $f(V) \sim V^2$, where V is the volume of a droplet. Also, this value is close to values of μ equal to 7 and 8 given in Table 1.4.

Cloud systems can easily cover an area $S \approx 10^3\,\mathrm{km}^2$ (Kondratyev and Binenko, 1984). So the total amount of water $W = wS$ (for idealized clouds having the same LWP for the whole cloudy area) stored in such a water cloud system is equal approximately to 10^8 kg, if we assume that $w = 100\ \mathrm{g/m}^2$, which is a typical value for cloudy media (see Fig. 1.6). This underlines the importance of clouds both for climate problems and human activity (e.g., crops production, flooding, etc.).

Table 1.5. The continental cloud model (CCM) and the marine cloud model (MCM) proposed to be used in combination with Eq. (1.3).

The cloud parameter	CCM	MCM
a_0, μm	4	6
μ	6	6
N, cm^{-3}	250	100

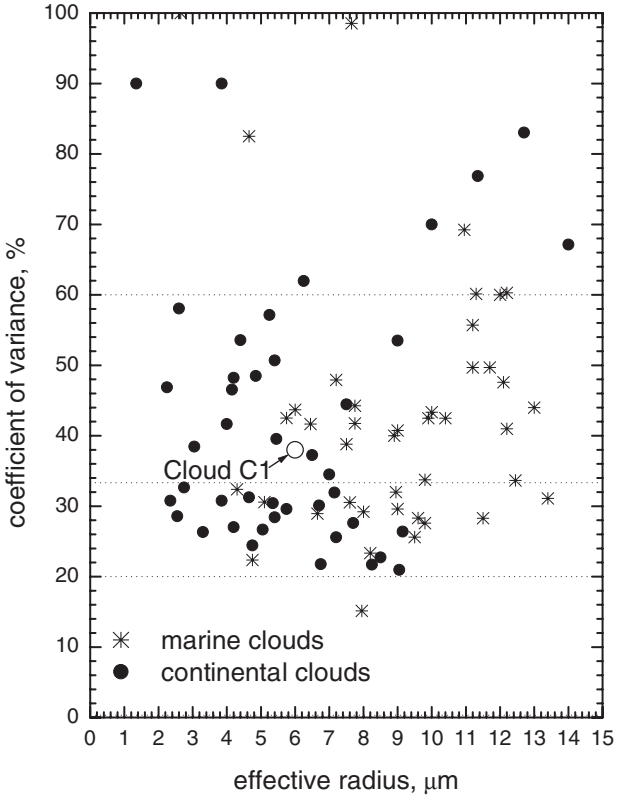

Fig. 1.17. Correlation between values of C and a_{ef} for marine and continental clouds.

1.1.2 Sizes and Shapes of Crystals

Microphysical properties of ice clouds cannot be characterized by a single PSD curve as in the case of liquid clouds even if one considers relatively small volumes of a cloudy medium. This is due to the extremely complex shapes of ice particles